

## Magnetic Field Penetration of Erosion-Switch Plasmas

Rodney J. Mason and Michael E. Jones

*Applied Theoretical Physics Division, Los Alamos National Laboratory, Los Alamos, New Mexico 87545*

John M. Grossmann and Paul F. Ottinger

*Naval Research Laboratory, Washington, D.C. 20375-5000*

(Received 28 June 1988)

Computer simulations demonstrate that the entrainment (or advection) of magnetic field with the flow of cathode-emitted electrons can constitute a dominant mechanism for the magnetic field penetration of erosion-switch plasmas. Cross-field drift in the accelerating electric field near the cathode starts the penetration process. Plasma erosion propagates the point for emission and magnetic field injection along the cathode toward the load—for the possibility of rapid switch opening.

PACS numbers: 52.75.Kq, 52.40.Hf, 52.60.+h, 52.65.+z

Plasma-erosion-opening switches (PEOS)<sup>1</sup> are central elements in new inductive-pulsed-power technology that permits the storage of electrical energy magnetically in association with currents, rather than electrostatically. The switches must conduct for a long period, and then open quickly for maximal transfer of power to a load. They are of growing utility in light-ion inertial-confinement fusion and radiation-effects simulation,<sup>2</sup> yet the essential physics of their operation is still under investigation. Plasma convection has long been recognized as important in alternative switch concepts.<sup>3</sup> Our Letter gives new simulation results showing that magnetic advection with the emission electrons can constitute a dominant mechanism for the field penetration of a PEOS.

Experiments performed on the GAMBLE accelerators at the Naval Research Laboratory (NRL) have demonstrated that the magnetic field deeply penetrates the fill plasma in a PEOS prior to its opening.<sup>4</sup> A field equal to the driving intensity is measured at depths at least sixty skin depths within the plasma, and well above the cathode surface. Yet, at a typical density of  $10^{13}$  electrons/cm<sup>3</sup> and an initial temperature of 5 eV the switch plasma is classically collisionless during the 50-ns rise time for the magnetic pulse that drives the experiments. This incongruity has motivated a strong interest in anomalous field-penetration mechanisms.<sup>5</sup>

Explicit particle-in-cell simulations at low densities ( $\leq 4 \times 10^{12}$  cm<sup>-3</sup>) have predicted that electrons cross switches in a narrow current channel.<sup>6,7</sup> Implicit plasma simulations<sup>8</sup> have been performed for more realistic densities,<sup>9,10</sup> with deep penetration of the driving magnetic field observed<sup>10</sup> for fill densities as high as  $6 \times 10^{13}$  cm<sup>-3</sup>. In this Letter we demonstrate for the first time that such deep penetration of the collisionless plasma can be accomplished by advection (or entrainment) of the driving magnetic field with emitted electrons from the cathode.

Our simulations were performed with the implicit code ANTHEM, used in its three-fluid mode, with the initial

plasma ions and electrons as the first two fluids, and the emission electrons as the third. The code's physics and equations are documented in Ref. 8; Ref. 9 describes our emission algorithm. Calculations were in cylindrical geometry. The azimuthal  $B_\theta$ , axial  $E_z$ , and radial  $E_r$  electromagnetic fields were calculated by the implicit moment method.<sup>8</sup> We considered the behavior of switches constructed with a fully conducting anode, and so  $E_z$  was zero at this electrode. With a high emission threshold (e.g., 300 keV/cm) the PEOS can open rapidly through the formation of a gap by the action of magnetic pressure gradients normal to the cathode.<sup>9</sup> But with zero emission threshold (now thought to be most likely for a cathode bombarded by fill plasma) opening is slower, and accompanied by deeper plasma penetration by the magnetic field.<sup>10</sup> Here, we explain the mechanism for this penetration.

We have carried out global simulations of the Fig. 1 idealization of a switch in use on the PBF AII accelerator at the Sandia National Laboratories. The actual

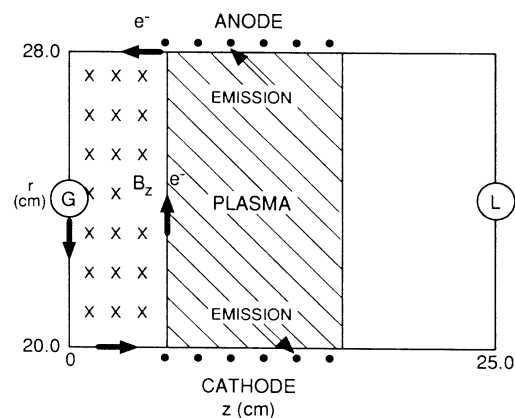


FIG. 1. A generic PEOS for inductive storage. Plasma initially fills the cross-hatched region. G denotes the generator and L the load, here a short circuit.

PBFAII switch is tapered with progressively smaller inner and outer radii in the direction of the load. Our cathode has a constant radius of 20 cm; its anode is at  $r=28$  cm. An  $E_r=0$  boundary condition was used for the short-circuit load  $L$  at  $z=25$  cm. A  $10^{13}$ -electrons/cm<sup>3</sup> plasma originally fills a region between the cathode and anode, while spanning the axial positions  $z=5.8$ – $15.3$  cm. We model a fully ionized  $C^{++}$  plasma, injected through the anode and towards the cathode at a speed  $v_r=6\times 10^6$  cm/s. A generator  $G$  at the left was simulated by setting  $B(z=0,r)=B_0(t)[(20\text{ cm})/r]$  with  $B_0(t)$  increasing linearly over 50 ns from 0 to 3 T, corresponding to a drive current rising to 3 MA. The simulations employed a  $50\times 50$  mesh with cell dimensions  $\Delta z=0.5$ ,  $\Delta r=0.16$  cm. The time step  $\Delta t$  was variable, and principally constrained by a Courant limit on the fastest electrons.

Our results are collected in Fig. 2. Frames 2(a)–2(d) plot axial cuts of the evolving  $B_\theta$  field for  $r$  at 20, 24, and 28 cm. Frame 2(e) shows contours of the early-time ( $t=12$  ns) penetration of the switch fill plasma by the  $B_\theta$  magnetic field component. Frame 2(i) shows electron density contours at the same instant. Frames 2(m)–2(p) give vector field plots of the total current density in the

At the perfectly conducting anode  $B_\theta$  accumu-

lates,<sup>6,9,10</sup> and approaching electrons are magnetically insulated. They propagate along the anode toward the load side of the plasma until the insulation is weak enough to allow their entry to the anode. Magnetic pressure pushes the plasma away from this electrode.  $B_\theta$  then propagates along it to the right, so that after 20.5 ns, 5% of the drive field is measured at the load. By 34.5 ns, 33% of the drive value is measured there.

At the cathode an electron gap is initiated by radial acceleration of electrons in the inductive  $E_r < 0$  field, and the  $B_\theta$  magnetic field penetrating the first few skin depths of the plasma. The emitted electrons are bent axially by the  $\mathbf{v}\times\mathbf{B}$  force, and undergo  $\mathbf{E}\times\mathbf{B}$  drift along the cathode until the resulting excess of positive charge pulls the rising jet of emission electrons back toward the generator—to run, at first, up along the generator side of the fill plasma. The charge excess also initiates ion erosion by accelerating ions toward the cathode. This reduces the local ion density, and with it, the electron density—starting a plasma erosion gap. Emitted electrons are magnetically insulated in the erosion gap, and the local skin depth expands, allowing more  $B_\theta$  to penetrate. The largest  $B_\theta$  gradients shift to the right edge of the gap. Through  $E_z \approx -(1/en_e)\partial(B_\theta^2/8\pi)/\partial z$ , the resultant magnetic pressure gradient (which is equivalent to a  $\mathbf{J}\times\mathbf{B}$  force) pushes axially on the ions at

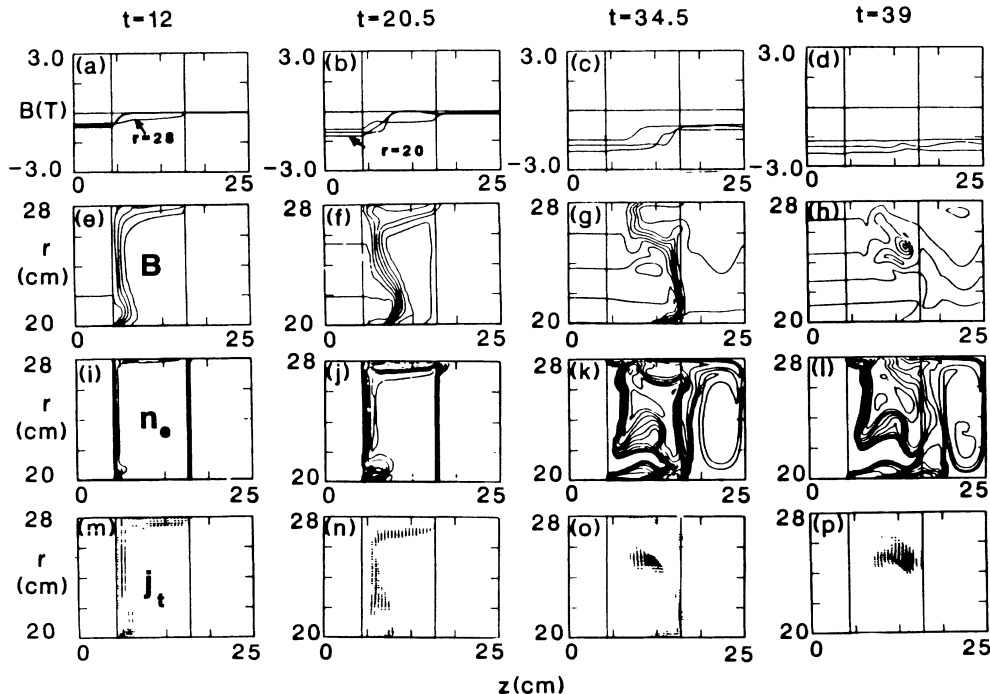


FIG. 2. Global collisionless calculation of the idealized PBFAII PEOS with  $10^{13}$ -cm<sup>-3</sup>  $C^{++}$  fill density, under a linear drive pulse rising to 3 T in 50 ns at the cathode. Frames (a)–(d) (and corresponding columns) are for  $t=12$ , 20.5, 34.5, and 39 ns, respectively. (a)–(d) Linear cuts of  $B_\theta(r,z)$  at  $r=20$  (cathode), 24 (body center), and 28 (anode) cm. (e)–(h) Corresponding  $B_\theta$  contour plots. (i)–(l) Total electron density contour plots, with the erosion gap and magnetic insulation visible at  $t=34.5$  and 39 ns. The eleven contour lines range logarithmically from  $10^{11}$  to  $3\times 10^{13}$  cm<sup>-3</sup>. (m)–(p) Total flux vector field,  $-j_e + Zj_i$ .

the cathode-gap corner. Here, the  $E_z$  field accelerates ions in a leaky piston, accelerating toward the load,<sup>7</sup> and shocking the ions to a density at least twice its initial value. The resultant decrease in skin depth further steepens the magnetic field gradients. When  $E_r$  is forced to zero at the cathode by emission, Ampere's law dictates that the electron current obeys  $j_e = -(c/4\pi) \partial B_\theta / \partial z - j_i$ , extracting the strongest electron emission at the gap edge. Thus, as the erosion gap opens, the point for maximal electron emission marches across the cathode toward the load.

The progress of its motion is recorded in frames 2(i)–2(l). The right side of the erosion gap has arrived within a skin depth of the original load-side edge of the fill plasma at 35 ns. Rapid filling of the load region with  $B_\theta$  proceeds in the next 5 ns. Electrons continue to emit along the full length of the cathode originally exposed to the fill plasma (the only region over which emission was permitted in the calculation), but magnetic insulation confines them to within a centimeter of the cathode. An electron gap in which  $n_e$  is less than  $10^{11} \text{ cm}^{-3}$  is evident up to 2.5 cm above the cathode at  $t=39$  ns. Corresponding contours of the ion density show a similar gap, but with no ion accumulation at the cathode surface. The concept of switch opening through an erosion gap formed the bases of early PEOS models.<sup>1,2</sup>

In the *body* of the fill plasma over time scales  $\tau$  such that  $\omega_p \tau \gg 1$  (with  $\omega_p$  the local plasma frequency), the collisionless electron momentum equation reduces<sup>8–10</sup> to  $\mathbf{E} \approx -\mathbf{v} \times \mathbf{B}/c$ , from which Faraday's law yields

$$\partial B_\theta / \partial t = -\partial(v_{ez} B_\theta) / \partial z - \partial(v_{er} B_\theta) / \partial r + \dots$$

[The largest of the remaining terms represents a separation of the magnetic field lines from the electrons entraining them over several skin depths—as evident from

the complete equation, Ref. 8, Eq. (23).] At large  $r$  this is analogous to the continuity equation for the advection of electron density. Thus,  $B_\theta$  is delivered by advection along the moving electron current channel, as it marches with the erosion gap along the cathode towards the load. The rate of delivery into the plasma body can be large, since  $v_e \rightarrow c$ , the speed of light (crossing 30 cm every nanosecond).  $B_\theta$  can accumulate with electron flow stagnation near the anode. Also, missing of the injected emission electron stream with the background electrons can result in  $B_\theta$  deposition, and inertia can leave  $B_\theta$  behind, when the current channel direction changes abruptly. Additional  $B_\theta$  penetration occurs across the extended skin depth in the low-density plasma above the erosion gap [see frame 2(k)]. However, in both 2(j) and 2(k) advection was crucial to transport  $B_\theta$  across the dense fill plasma near, for example,  $r=23$  cm.

When the same switch configuration is simulated with infinite-mass ions so that no erosion gap can form, opening is still achieved as documented by Fig. 3. By 34.5 ns, nearly comparable currents pass through the load as in the finite-mass (Fig. 2) study. The subsequent rapid-opening phase (associated with breakthrough of the field via the cathode erosion gap) is, however, lacking. Thus, we must wait until 60 ns (not shown) for full opening with fixed ions. The emission point remains attached to the generator-cathode corner of the fill plasma, and a broader current channel evolves from the fixed electron emission point. Still,  $\mathbf{v} \times \mathbf{B}$  deflects the emission, carrying the current sheet and the advected  $B_\theta$  at midswitch radii across nearly 5 cm of fill plasma by 35 ns.

Finally, to verify that advection is responsible for the deep transport of the magnetic field, in the calculations for Fig. 4 we have suppressed the advection, by zeroing out the  $\mathbf{v} \times \mathbf{B}$  terms in our plasma and implicit field up-

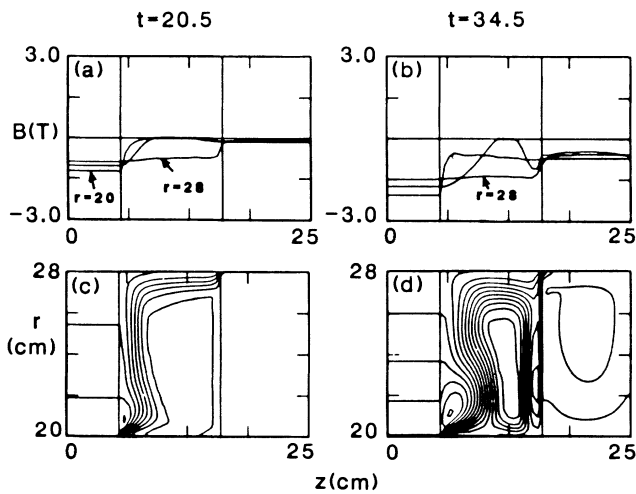


FIG. 3.  $B_\theta$  penetration with fixed ions. Cuts [as in Figs. 2(a)–2(d)] and contours for (a),(c) 20.5 ns and (b),(d) 34.5 ns.

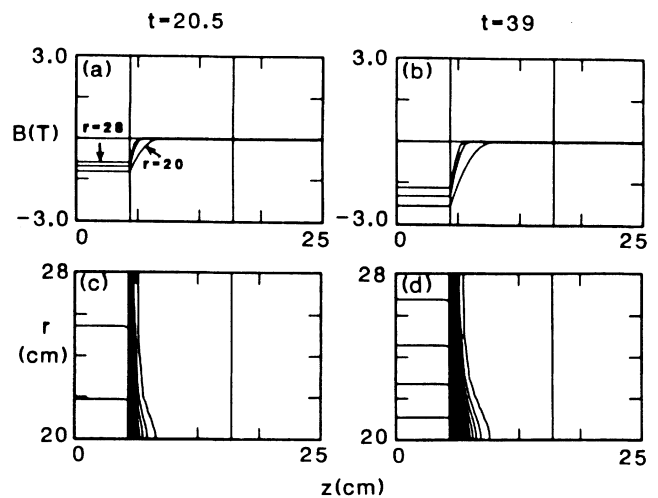


FIG. 4. Significantly reduced  $B_\theta$  penetration when  $\mathbf{v} \times \mathbf{B}$  terms are suppressed (with fixed ions) in the plasma and implicit field update calculations. (a),(c) 20.5 ns; (b),(d) 39 ns.

date calculations (still with  $m_i/m_e \rightarrow \infty$ ). As expected, only a generator-side surface current is calculated; deep field penetration of the fill plasma ceases.

Thus, we determined that advection with the electron emission stream can lead to the deposition of a substantial magnetic field in the fill-plasma body of a PEOS, with no anomalous resistivity employed. Resultant conduction and opening times (34 ns and 5 ns, respectively) are consistent with experimental experience on the PBF-II accelerator. The  $\mathbf{v} \times \mathbf{B}$  deflection of the emitted electrons in the accelerating radial electric field near the cathode starts the formation of a gap which continues to open by erosion, resulting in deep penetration of the plasma by the emission current sheet, and accompanying an advected magnetic field. Switch opening (to a short-circuit load) can occur gradually (over  $\sim 50$  ns through 10 cm of a  $10^{13}\text{-cm}^{-3}$  fill plasma) along the anode, even with fixed ions, or quickly ( $\sim 5$  ns) as the erosion gap breaks through to the load side of the fill plasma at the cathode.

There still remains a need for better agreement with broad-current-sheet data seen in early NRL experiments.<sup>4</sup> Broader current sheets (and broader  $B_\theta$  transitions) may follow directly at high density from a particle (rather than fluid) treatment of the plasma.<sup>11</sup> Alternatively, as with our earlier fluid modeling,<sup>9,10</sup> some inclusion of anomalous resistivity may still be necessary to match the sheet-width data. Advection will transport magnetic field into the PEOS in concert with any such additional effects.

We acknowledge stimulating discussions with D. Winske, J. Wallace, and J. Paquin at Los Alamos National Laboratory, C. Mendel, J. Quintenz, and M. A. Sweeney at Sandia National Laboratory, and P. Steen

and A. Wilson at Maxwell Laboratories. This work was performed under the auspices of the U.S. Department of Energy.

---

<sup>1</sup>R. A. Meger, R. J. Commisso, G. Cooperstein, and S. A. Goldstein, *Appl. Phys. Lett.* **42**, 943 (1983); P. F. Ottinger, S. A. Goldstein, and R. A. Meger, *J. Appl. Phys.* **56**, 774 (1984).

<sup>2</sup>G. Cooperstein and P. F. Ottinger, *IEEE Trans. Plasma Sci.* **15**, 629 (1987).

<sup>3</sup>P. J. Turchi, in *Opening Switches*, edited by A. Gunther, M. Kristiansen, and T. Martin (Plenum, New York, 1987), p. 191.

<sup>4</sup>B. V. Weber, R. J. Commisso, R. A. Meger, J. M. Neri, W. F. Oliphant, and P. F. Ottinger, *Appl. Phys. Lett.* **45**, 1043 (1984).

<sup>5</sup>R. Kulsrud, P. F. Ottinger, and J. M. Grossmann, *Phys. Fluids* **31**, 1741 (1988); S. S. Payne, T. W. Hussey, R. W. Stinett, and N. F. Roderick, *IEEE Trans. Plasma Sci.* **15**, 725 (1987).

<sup>6</sup>E. M. Waisman, P. G. Steen, D. E. Parks, and A. Wilson, *Appl. Phys. Lett.* **46**, 1045 (1985).

<sup>7</sup>J. M. Grossmann, P. F. Ottinger, J. M. Neri, and A. T. Drobot, *Phys. Fluids* **29**, 2724 (1986).

<sup>8</sup>R. J. Mason, *J. Comput. Phys.* **71**, 429 (1987).

<sup>9</sup>R. J. Mason, J. M. Wallace, J. M. Grossmann, and P. F. Ottinger, *IEEE Trans. Plasma Sci.* **15**, 715 (1987).

<sup>10</sup>R. J. Mason, M. E. Jones, J. M. Grossmann, and P. F. Ottinger, Los Alamos Report No. LA-UR-87-3553, 1988 (unpublished), and *J. Appl. Phys.* (to be published).

<sup>11</sup>R. J. Mason and M. E. Jones, Los Alamos Report No. LA-UR-88-2029 (unpublished), and in the Proceedings of the Seventh International Conference on High Power Particle Beams, 4-8 July 1988, Karlsruhe, Federal Republic of Germany (to be published).

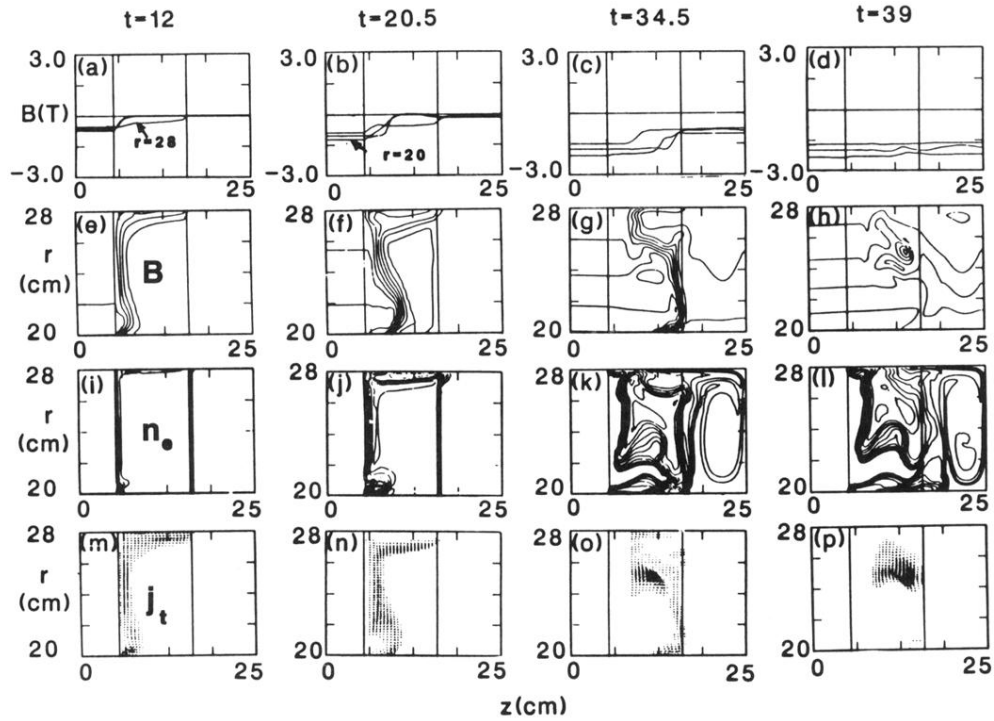


FIG. 2. Global collisionless calculation of the idealized PBFAII PEOS with  $10^{13}\text{-cm}^{-3}$   $\text{C}^{++}$  fill density, under a linear drive pulse rising to 3 T in 50 ns at the cathode. Frames (a)–(d) (and corresponding columns) are for  $t = 12, 20.5, 34.5,$  and  $39$  ns, respectively. (a)–(d) Linear cuts of  $B_\theta(r, z)$  at  $r = 20$  (cathode), 24 (body center), and 28 (anode) cm. (e)–(h) Corresponding  $B_\theta$  contour plots. (i)–(l) Total electron density contour plots, with the erosion gap and magnetic insulation visible at  $t = 34.5$  and  $39$  ns. The eleven contour lines range logarithmically from  $10^{11}$  to  $3 \times 10^{13} \text{ cm}^{-3}$ . (m)–(p) Total flux vector field,  $-j_e + Zj_i$ .